Neuro-Oncology Advances

8(1), vdag070, 2026 | https://doi.org/10.1093/noajnl/vdag070 | Advance Access publication March 11, 2026

Disrupted transporter protein expression and cell-specific localization reveal neurovascular unit remodeling in human glioblastoma

Xun Bao[†], **Yuanyuan Jiang**[†], **Beth Hermes, Nader Sanai, and Jing Li**

All author affiliations are listed at the end of the article

Corresponding Author: Jing Li, PhD, Karmanos Cancer Institute, Wayne State University School of Medicine, 4100 John R Street, HWCRC, Room 523, Detroit, MI 48201, USA (lijing@wayne.edu).

[†]These are contributed equally and share first authorship of this work.

Abstract

Background. Current understanding of transporter protein expression and localization within the neurovascular unit (NVU) of the human normal brain cortex and glioblastoma (GBM) remains largely qualitative and lacks cellular resolution. This study aimed to provide a quantitative characterization of transporter protein expression and cell-specific localization in the NVU of normal brain cortex and GBM.

Methods. Protein expression of major ATP-binding cassette transporters and solute carrier transporters was quantified in microvessels isolated from distinct regions of the human normal brain cortex and GBM using LC-MS/MS–based targeted proteomics. NVU structure and cell-specific transporter localization were visualized and quantitatively assessed by high-resolution confocal immunofluorescence microscopy.

Results. Targeted proteomics revealed marked alterations in transporter protein abundance in microvessels isolated from both non-enhancing and enhancing regions of GBM, compared with normal brain cortex. ATP-binding cassette (ABC) efflux transporters (ABCB1, ABCG2) were largely preserved. Ion and nutrient transporters (Na^+/K^+-ATPase, GLUT3, EAAT1, EAAT2, SNAT2) were significantly reduced (ANOVA, $P<.05$). GLUT1 appeared downregulated while not reaching statistical significance. LAT1 and SNAT3 protein abundance was significantly increased (ANOVA, $P<.05$). Confocal immunofluorescence microscopy demonstrated a well-organized NVU architecture in normal brain cortex and a markedly disorganized structure in GBM. Quantitative co-localization analyses identified distinct, cell-type specific transporter distribution patterns in the normal NVU, contrasted by diffuse and mislocalized transporter expression in GBM NVU.

Conclusions. GBM drives profound NVU remodeling at both molecular and structural levels. Disruption of transporter protein expression and cell-specific localization likely contributes to pharmacokinetic heterogeneity, metabolic plasticity, and invasive phenotype of GBM.

Key Points

- NVU remodeling at both structural and molecular levels in glioblastoma (GBM).
- Disrupted transporter protein expression and cellular localization in GBM neurovascular unit.
- Transporter disruption driving PK heterogeneity and metabolic plasticity in GBM.

Received November 24, 2025; accepted March 3, 2026.

Importance of the Study

This study reveals key molecular and structural mechanisms underlying neurovascular unit (NVU) remodeling in human glioblastoma (GBM). Disrupted transporter protein expression and cellular localization indicate a breakdown of the coordinated neurovascular and metabolic coupling, contributing to pharmacokinetic heterogeneity, metabolic plasticity, and invasiveness of GBM. In contrast-enhancing regions, disorganized NVU structural and mislocalized ATP-binding cassette efflux transporters lead to diminished or absent active efflux function at the blood-brain barrier, consistent with clinically observed enhanced drug penetration into these regions. In non-enhancing regions, the relatively preserved NVU structure and efflux transporter expression likely lead to therapeutic resistance. Marked dysregulation of nutrient and ion transporters across non-enhancing and enhancing regions suggests that biochemical barrier alterations may precede overt NVU structural disruption. These early molecular changes likely facilitate metabolic reprogramming of infiltrative tumor cells. Therapeutic strategies that target both NVU dysfunction and transporter dysregulation may improve drug delivery and harness metabolic vulnerability in GBM.

The three-dimensional structure of the neurovascular unit (NVU) is a highly organized, multicellular interface that surrounds the brain's microvasculature, ensuring the integrity and function of the blood-brain barrier (BBB).[1] At its core lies a capillary composed of a monolayer of brain microvascular endothelial cells tightly connected by junctional complexes, forming a selective barrier between the blood and the brain parenchyma.[1] These endothelial cells are embedded within a shared basement membrane that also contains pericytes, which wrap around capillaries and support vascular stability and signaling.[1,2] Surrounding this core are astrocytic endfeet that ensheathe the capillary wall, regulating water and ion hemostasis through channels such as aquaporin-4.[1] Neurons and microglia interact with the NVU through chemical and metabolic signals. This intricate NVU structural arrangement enables precise regulation of cerebral blood flow, metabolic exchange, immune surveillance, and barrier function, all crucial for maintaining central nervous system homeostasis.[1,2]

In glioblastoma (GBM), the structure and function of the NVU are profoundly disrupted. GBM-derived vascular epithelial growth factor (VEGF) drives formation of leaky, disorganized vessels with poor perfusion and increased permeability.[3] BBB integrity becomes compromised due to disrupted tight junctions, abnormal angiogenesis, and reduced pericyte coverage.[3,4] Astrocytic endfeet retract or lose contact with the vasculature, impairing their regulatory roles, while microglia and infiltrating immune cells become activated and often support tumor progression.[1,3,4]

Transporter expression and localization within the NVU may be also altered in brain tumors, contributing to NVU remodeling. However, current knowledge on the expression of the ATP-binding cassette (ABC) efflux transporters and solute carriers in the NVU of both the human normal brain and GBM remains limited, largely qualitative. Most available studies rely on semi-quantitative immunohistochemistry or mRNA-based assays, which may yield inconsistent results due to variable antibody specificity, inadequately purified microvessel preparation, and well-recognized discordance between mRNA and protein expression levels.[5–7] Importantly, transporter function at the BBB and within the NVU is determined by protein abundance and localization rather than transcript levels. It has been demonstrated that mRNA expression does not reliably predict protein abundance, particularly for membrane proteins subject to complex post-transcriptional, translational, and post-translational regulation.[5,6]

Quantitative characterization of transporter protein expression within the NVU is therefore essential for understanding normal brain physiology, GBM pathophysiology, and therapeutic drug delivery to the brain and tumors. In this study, we used LC-MS/MS–based targeted proteomics to quantify the protein abundances of major ABC transporters and solute carriers in microvessels isolated from the human normal brain cortex, the non-cancerous cortex of glioblastoma patients, and paired contrast-enhancing and non-enhancing regions of GBM. In addition, we applied high-resolution confocal immunofluorescence microscopy to visualize and quantitatively assess cell-specific localization of transporters within specific cellular compartments of the NVU, including endothelial cells, pericytes, astrocytes, and neurons. These complementary approaches address distinct but interrelated aspects of transporter biology at the protein level. Collectively, this comprehensive analysis provides quantitative characterization on transporter protein expression and localization in the NVU of both the human normal brain cortex and GBM, offering critical insights into GBM-induced neurovascular remodeling and potential therapeutic implications.

Methods

Human Normal Brain Cortex Specimens and Non-cancerous Brain Cortex Specimens of Glioblastoma Patients

Normal brain cortex specimens were obtained from 12 donors (from 2 Brodmann areas) who died from natural causes or accidents and had no history of neuropathological diseases. Non-cancerous brain cortex specimens were sourced from 11 GBM patients (from 4 Brodmann areas) who succumbed to the disease. All specimens were provided by the NeuroBioBank Brain and Tissue Repositories of National Institute of Health (Bethesda, MD) under a Material Transfer Agreement. Detailed demographic information, health status, and cause of death for the donors can be found in Tables S1 and S2.

Human Glioblastoma Specimens

GBM specimens, including paired contrast-enhancing and non-enhancing regions, were intraoperatively collected from 25 patients during tumor resection at Barrow Neurological Institute under an IRB-approved tissue collection protocol (#05TS038). In brief, the locations of enhancing and non-enhancing tumor areas were identified with an intraoperative MRI neuronavigation system. Approximate 0.1-1.0 g tissue per specimen were collected, snap-frozen in liquid nitrogen, and stored at –80°C until further analyses. Detailed demographic information, diagnosis, and disease/treatment history of the patients are provided in Table S3.

LC-MS/MS–based Targeted Quantitative Proteomics

Microvessels were isolated from normal brain cortex, non-cancerous cortex, and GBM tumor specimens using our optimized nylon mesh method.[8] Protein abundances of major ABC efflux transporters, amino acid transporters, and other solute carriers in isolated microvessels were determined using a validated LC-MS/MS–based targeted proteomics method, adapted from our published method.[8] Additional experimental details are provided in Supplementary Methods.

The transporters selected for our targeted proteomics analysis were based on evidence of BBB expression from immunohistochemistry, real-time polymerase chain reaction, or targeted proteomics. The panel included ABC efflux transporters (ABCB1, ABCG2, ABCC4), amino acid transporters (SLC1A1, SLC1A2/EAAT2, SLC1A3/EAAT1, SLC1A5, SLC6A14, SLC7A1, SLC7A3, SLC7A5/ L-type amino acid transporter 1 (LAT1), SLC7A11, SLC29A1/ENT1, SLC38A2/SNAT2, and SLC38A3/SNAT3), other solute carriers (OATP1A2, OATP2B1, OAT3, GLUT1, GLUT3), and Na+/K+-ATPase (plasma membrane marker). The probe peptides for individual transporters were selected from hypothetical trypsin digests based on in-silico selection criteria. Stable isotope-labeling of internal standards was achieved using ^{13}C and ^{15}N for amino acid labeling. All probe peptides and isotope-labeled internal standards (Table S4) were purchased from Thermo Scientific. To achieve optimal sensitivity, the proteomics workflow was divided into two panels, each monitoring ~100 transitions to quantify 10-12 transporters. Panel A measured ABC transporters, OATPs, OAT3, GLUT1, GLUT3, LAT1, and Na^+/K^+-ATPase; Panel B quantified a broad set of amino acid transporters. Assay performance metrics for both panels are summarized in Table S5.

Because the amount of human brain cortex and GBM tissue was limited, isolated microvessel samples were often insufficient to analyze both transporter panels. We therefore first quantified Panel A transporters in a larger batch consisting of 24 normal cortex specimens (12 donors, two Brodmann areas each), 29 non-cancerous cortex specimens from 11 GBM patients, and 21 GBM specimens (10 matched non-enhancing/enhancing pairs plus one non-enhancing tumor). As additional tissue became available, we performed a smaller batch analysis for Panel B transporters, which included 10 normal cortex specimens, 10 non-cancerous cortex specimens from GBM patients, and 7 GBM specimens (including three matched non-enhancing and contrast-enhancing pairs plus one non-enhancing tumor). Of note, although we enrolled 25 GBM patients and collected matched non-enhancing and enhancing tumor regions from each, variable and limited tissue yields required pooling samples from 2 to 3 patients to obtain sufficient material for microvessel isolation. Consequently, the final dataset comprised 10 matched tumor pairs and one additional non-enhancing tumor sample. Transporter abundances represent the average expression across the 2-3 tumors pooled into each sample. Details of pooled specimens are provided in Table S3.

Immunoblotting

Immunoblotting to assess the protein expression of Panel A and B transporters in leftover normal brain cortex microvessel samples that were previously analyzed by targeted proteomics. Experimental details and antibody information are provided in Supplementary Methods and Table S6.

Confocal Immunofluorescence Microscopy

Confocal immunofluorescence microscopy was employed to visualize and quantitatively assess the subcellular localization of transporters that were detectable by both targeted proteomics and immunoblotting. These included ABCB1, ABCG2, GLUT1, GLUT3, Na^+/K^+-ATPase, LAT1, SLC1A2, SLC1A3, SLC29A1, and SLC38A3. Localization was assessed in specific cellular compartments of freshly isolated brain and GBM microvessels, using well-established lineage markers: platelet endothelial cell adhesion molecule-1 (PECAM-1 or CD31) for endothelial cells, glial fibrillary acidic protein (GFAP) for astrocytes, neural/glial antigen 2 (NG2) for pericytes, and synaptophysin (SYP) for neurons.[9–12] These markers are extensively used in studies of the neurovascular unit and provide well-established specificity for identifying individual cellular components within brain microvascular preparations.[9–12] The observed co-localization of transporters with these validated markers provides strong evidence supporting transporter localization in the corresponding cell types. Importantly, the use of freshly isolated microvessels preserves the native structural and cellular organization of the neurovascular unit, allowing direct assessment of transporter localization under physiologically relevant conditions. This approach minimizes potential artifacts associated with cell dissociation, in vitro culture, or phenotypic alterations that may occur during isolation and propagation of individual cell types.

Detailed information on the primary and secondary antibodies used is provided in Table S7. The procedure for immunofluorescence staining of microvessels is described in Supplementary Methods. Of note, given the limited amount of microvessels isolated from each human normal brain cortex and especially GBM tissue specimens, isolated microvessels from 5 normal brain cortex specimens or 10 GBM enhancing tumor specimens were combined and used for immunofluorescence staining and microscopy analysis for 4 cell types and 10 transporters and their co-localization.

Confocal Z-stacks were acquired on a Zeiss LSM 780 microscope using a 63× oil-immersion objective, with optical sections collected at 0.6 µm intervals for precise 3D localization. Image analysis was performed in Volocity (Quorum Technologies Inc.) to quantify co-localization between transporters and cellular markers. Z-stack images were inspected to select representative 3D images. To ensure reproducibility, all imaging parameters, including laser power, gain, background subtraction and signal thresholding, were applied uniformly across all images during image acquisition and processing. Regions of interest encompassing NVU microvascular structures were manually defined using cell-specific markers (CD31 for endothelial cells, GFAP for astrocytes, NG2 for pericytes, SYP for neurons). Maximum intensity values were obtained for transporter (Channel 1) and cell marker (Channel 2) signals, and a 25% threshold was applied to each channel. Co-localization was quantified using Mander's overlap coefficients (M1 and M2) and Pearson's correlation coefficient.[13,14] M1 reflects the fraction of transporter signal overlapping the cell marker, and M2 reflects the reverse; both range from 0 to 1. Pearson's coefficient assesses correlation of signal intensities between two channels.

Statistical Analysis

Statistical differences in the abundance of individual transporter proteins between groups were assessed using ordinary one-way ANOVA followed by Tukey's post hoc multiple comparisons test. A multiplicity-ANOVA, $P < .05$ was considered statistically significant. All analyses were conducted using GraphPad Prism version 10.4.1.

Results

Microvessel Morphology and Recovery

The morphology of microvessels from normal brain cortex, non-cancerous cortex of GBM patients, and GBM tissue was examined by microscopy (Figure 1A-D). Normal and non-cancerous cortical microvessels were small, well-organized, and displayed smooth, regular branching (Figure 1A and B). In contrast, GBM microvessels were frequently tortuous, dilated, and disorganized, with irregular branching patterns (Figure 1C and D), reflecting pathological angiogenesis driven by tumor-associated hypoxia and rapid proliferation.

Microvessel recovery, expressed as microgram protein per gram of tissue (µg/g), from normal cortex, non-cancerous cortex of GBM patients, and GBM tumor regions is summarized in Figure 1E. Median microvessel recovery (with 95% confidence intervals) was 246 µg/g (218-309) in normal brain cortex, 161 µg/g (136-203) in non-cancerous cortex of GBM patients, and 137 µg/g (120-215) in GBM tumor tissue. Substantial inter-individual and regional variability in recovery was observed, consistent with the inherent heterogeneity of vascular density in the human brain and GBM. Microvessel recovery from Brodmann area 21 of the non-cancerous cortex in GBM patients was significantly lower than Brodmann areas 44 and 47 of normal brain cortex (ANOVA, $P<.01$). Recovery from enhancing GBM regions was significantly lower than Brodmann area 44 of the normal brain (ANOVA, $P<.01$). Overall, microvessel recovery from GBM tumor tissue was significantly reduced compared to normal brain cortex (ANOVA, $P<.01$), reflecting the disrupted vascular architecture and heterogeneous vessel density in GBM.

Quantitative Transporter Protein Expression in Isolated Microvessels

Quantitative abundances of Panel A and B transporters in microvessels from normal cortex, non-cancerous cortex of GBM patients, and GBM tumor regions are summarized in Figure 2 and Table 1. Considerable inter-individual and regional variability was observed for Panel A transporters (ABCB1, ABCG2, Na^+/K^+-ATPase, GLUT1, GLUT3, LAT1) and Panel B transporters (SLC1A2/EAAT2, SLC1A3/EAAT1, SLC7A5/LAT1, SLC29A1/ENT1, SLC38A2/SNAT2, SLC38A3/SNAT3). Other transporters in Panel A (ABCC4, OATP1A2, OATP2B1, OAT3) and Panel B (SLC1A5, SLC6A14, SLC7A1, SLC7A3, SLC7A11) were below the quantitation limit in all samples.

Despite inter- and intra-individual variability, transporter abundances in microvessels from the non-cancerous cortex of GBM patients were generally similar to normal cortex, indicating largely preserved NVU biochemical barrier function (Figure 2 and Table 1). In contrast, microvessels from non-enhancing and contrast-enhancing regions of GBM showed marked alterations and increased variability. Specifically, the abundances of Na^+/K^+-ATPase, GLUT3, SLC1A2 (EAAT2), SLC1A3 (EAAT1), SLC38A2 (SNAT2), and SLC38A3 (SNAT3) were significantly reduced in tumor microvessels (ANOVA, $P<.05$), whereas SLC7A5 (LAT1) and SLC38A3 (SNAT3) were significantly upregulated (ANOVA, $P<.05$). GLUT1 protein abundance was decreased while not reaching statistical significance. The levels of ABCB1 and ABCG2 remained comparable to those in normal brain cortex microvessels. Of note, although transporter abundances varied between matched non-enhancing and enhancing tumor specimens from individual patients (Figure S1), the overall mean and median abundances were similar between these two regions (ANOVA, $P>.05$) (Table 1).

Notably, ABCB1/ABCG2 protein abundances in microvessels from normal brain cortex or non-tumor cortex measured in the present study fall within the ranges reported in our previous studies,[8,15] despite at a relative lower mean level in the present study, which may reflect biological inter- and intra-individual variability among specimens rather than methodological differences. In this study, normal brain cortex specimens were obtained from 12 donors (from two Brodmann areas), and non-cancerous brain cortex specimens were sourced from 11 GBM patients (from four Brodmann areas). In contrast, in our previous studies, information on Brodmann areas was unavailable, and specimens were likely derived from multiple different brain regions, which may have contributed to variability in measured transporter levels. It should also be emphasized that a standardized quality control sample of cells (i.e., MDCKII cells with stable expression of ABCB1) has been included in all batches

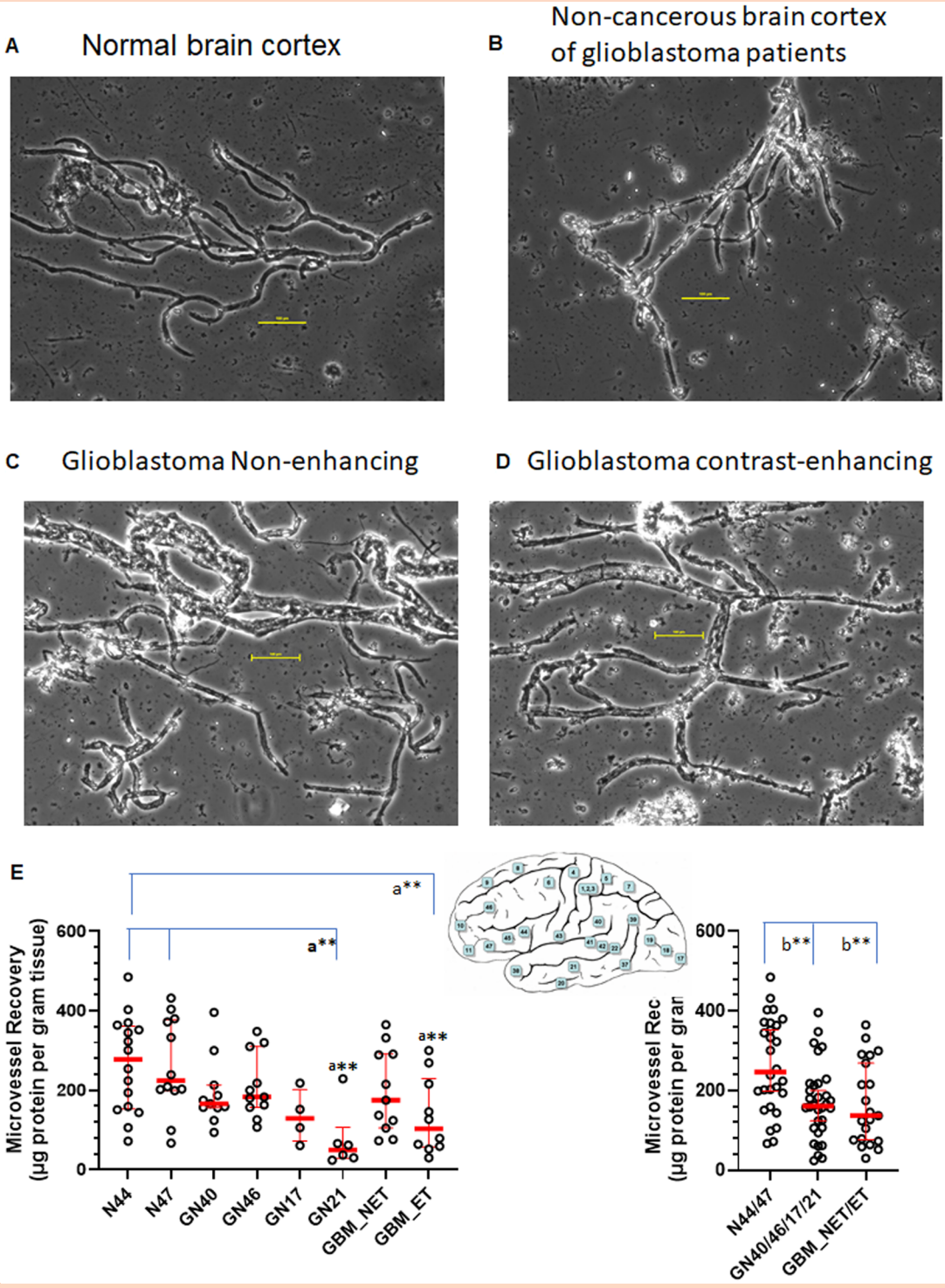

Figure 1 Microscopy images of microvessels isolated from (A) the human normal brain cortex, (B) non-cancerous cerebral cortex of glioblastoma (GBM) patients, (C) non-enhancing region of GBM, and (D) contrast-enhancing region of GBM. (E) Microvessel recovery from distinct regions of normal brain cortex (Brodmann areas 44 and 47), non-cancerous cerebral cortex (Brodmann areas 40, 46, 17, and 21) of GBM patients, as well non-enhancing and contrast-enhancing regions of GBM. Scale bar = 100 µm. [a]Microvessel recovery from Brodmann area 21 of the non-cancerous cortex in GBM patients was significantly lower than recovery from Brodmann areas 44 and 47 in normal brain cortex ($P < .01$, ordinary one-way ANOVA followed by Tukey's post hoc multiple comparisons test). [b]Microvessel recovery from enhancing GBM regions was significantly lower than from Brodmann area 44 of the normal brain (ANOVA, $P < .01$). Overall, microvessel recovery from both non-cancerous cortex and GBM tumor tissue was significantly reduced compared to normal brain cortex ($P < 0020.01$, ordinary one-way ANOVA followed by Tukey's post hoc multiple comparisons test).

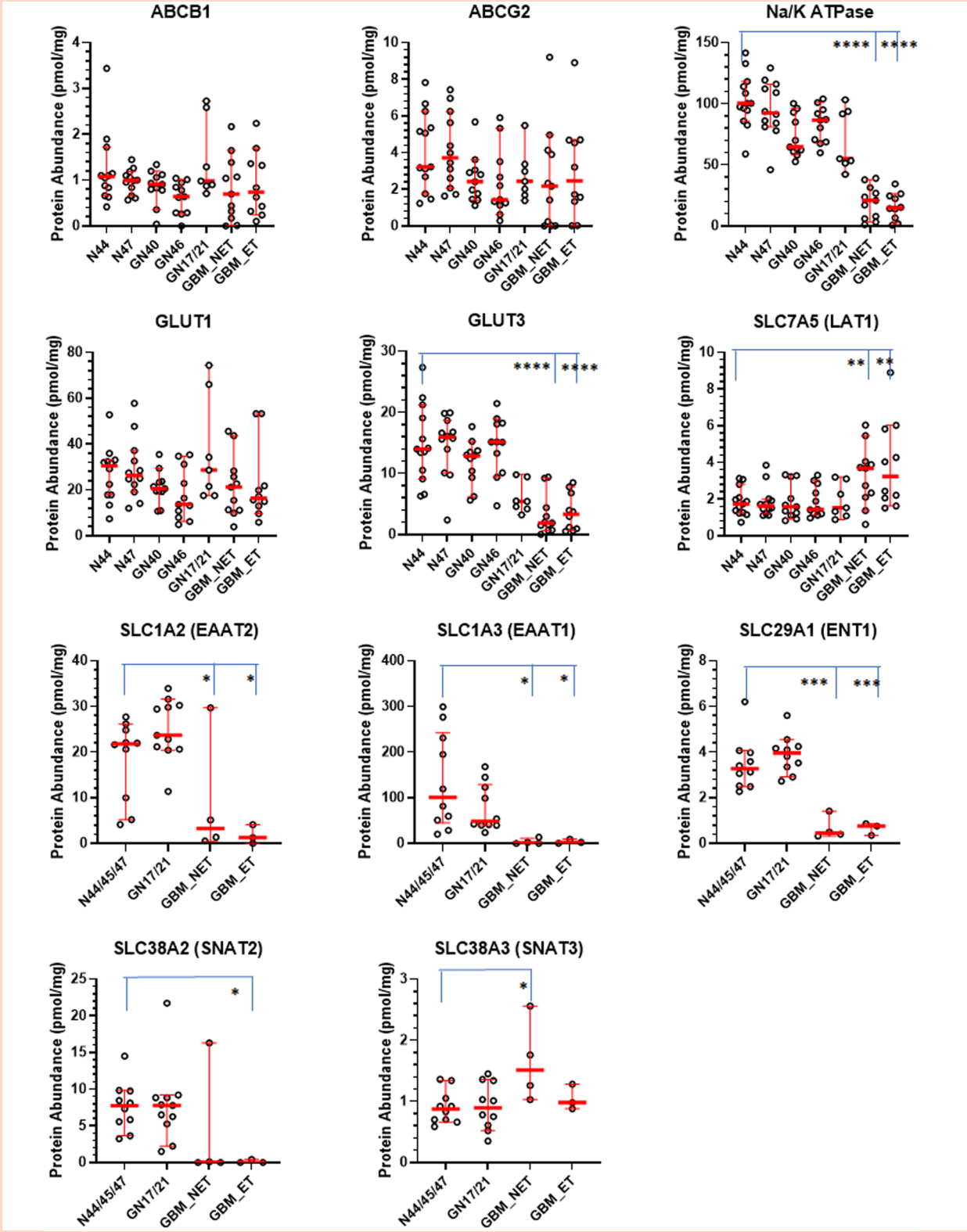

Figure 2 Comparative protein abundances (pmol/mg) of major transporters in microvessels isolated from distinct regions of the human normal brain cortex (Brodmann areas 44 and 47), non-cancerous cerebral cortex (Brodmann areas 40, 46, 17, and 21) of GBM patients, as well non-enhancing and contrast-enhancing regions of GBM. Symbols represent individual sample measurements. Lines and error bars represent the median and 95% confidence interval. Ordinary one-way ANOVA followed by Tukey's post hoc multiple comparisons test: $^{****}P<.0001$, $^{***}P<.001$, $^{**}P<.01$, $^{*}P<.05$.

Table 1. Transporter protein abundances (fmol/μg protein)[a] in the microvessels isolated from the human normal brain cortex, non-cancerous cortex of glioblastoma patients, as well as non-enhancing and enhancing regions of glioblastoma

	N44[b]	N47[b]	GN40[c]	GN46[c]	GN17/21[c]	GBM_NET[d]	GBM_ET[d]
Number of samples	12	12	11	11	7	11	10
ABCB1	1.075 (0.42-3.44)	0.995 (0.57-1.45)	0.91 (0.04-1.34)	0.64 (BLQ-1.04)	0.98 (0.71-2.73)	0.7 (BLQ-2.17)	0.735 (0.1-2.24)
ABCG2	3.23 (1.24-7.83)	3.72 (1.64-7.44)	2.42 (1.12-5.68)	1.44 (0.29-5.91)	2.44 (1.39-5.49)	2.17 (BLQ-9.21)	2.465 (0.01-8.91)
Na/K ATPase	100.5 (58.88-141.7)	92.58 (46.09-129.4)	64.73 (52.71-100.3)	86.59 (59.98-104.1)	55.06 (42.36-103.4)	20.91 (1.22-39.12)	14.82 (0.74-34.49)
GLUT1	30.56 (7.45-52.83)	26.31 (12.05-57.83)	20.55 (10.77-35.51)	13.7 (4.89-35.35)	28.72 (17.55-74.45)	21.25 (3.94-45.62)	16.38 (5.89-53.39)
GLUT3	13.98 (6.32-27.37)	15.93 (2.39-19.93)	12.89 (5.63-17.68)	15.17 (4.72-21.46)	5.44 (3.23-9.8)	1.92 (0.03-9.41)	3.345 (0.54-8.52)
SLC7A5 (LAT1)	1.74 (0.74-3.13)	1.62 (1.11-3.85)	1.59 (0.83-3.33)	1.44 (0.97-3.3)	1.53 (0.89-3.2)	3.68 (0.62-6.04)	3.24 (1.51-8.9)

	N44/45/47[b]	GN17/21[c]	GBM_NET[d]	GBM_ET[d]
Number of samples	10	10	4	3
SLC1A2 (EAAT2)	21.82 (4.16-27.71)	23.73 (11.4-33.98)	3.265 (0.56-29.73)	1.29 (BLQ-4.13)
SLC1A3 (EAAT1)	100.7 (20.46-299.4)	48.41 (23.82-168.2)	1.19 (BLQ-13.89)	2.41 (0.47-9.56)
SLC29A1 (ENT1)	3.27 (2.28-6.21)	3.965 (2.73-5.61)	0.455 (0.32-1.42)	0.76 (0.36-0.86)
SLC38A2 (SNAT2)	7.735 (3.24-14.51)	7.78 (1.51-21.73)	0.055 (BLQ-16.32)	0.02 (BLQ-0.43)
SLC38A3 (SNAT3)	0.875 (0.59-1.36)	0.895 (0.35-1.45)	1.51 (1.03-2.56)	0.98 (0.88-1.28)

[a]Data are shown as the median (with the minimum-maximum).
[b]N44, N45, N47, the human normal brain cortex specimens collected from Brodmann areas 44, 45, and 47.
[c]GN40, GN46, GN17/21, the non-cancerous cortex specimens of glioblastoma patients collected from Brodmann areas 40, 46, 17, and 21.
[d]GBM_NET and GBM_ET, non-enhancing and contrast-enhancing regions of glioblastoma specimens.

of proteomic analyses in both the present and previous studies. The measured transporter levels (represented by ABCB1, Na^+/K^+-ATPase, and GLUT1) were highly consistent across two studies (Table S8), thereby reinforcing confidence in the reproducibility of the assay.

ABCB1 and ABCG2 abundances in microvessels from both enhancing and non-enhancing GBM regions were comparable to those in normal and non-cancerous cortex (Figure 2 and Table 1), contrasting with our previous study reporting reduced levels.[15] Both studies used the same targeted proteomics protocol, with consistent ABCB1 and ABCG2 measurements in normal brain cortex microvessels, highlighting methodological reproducibility. The discrepancy in the results from two studies likely reflects differences in specimen quality. In this study, paired tumor regions of GBM were intraoperatively collected, snap-frozen, and stored less than 2 years, whereas prior specimens were biobank-derived with variable, prolonged storage (3-10 years), potentially causing protein degradation and artificially low measurements of ABCB1 and ABCG2 in GBM microvessels.

Immunoblotting of Transporters in Microvessels

Immunoblotting of leftover microvessel samples confirmed the presence of Panel A and B transporters detected by targeted proteomics, including ABCB1, ABCG2, Na^+/K^+-ATPase, GLUT1, GLUT3, LAT1, SLC1A2/EAAT2, SLC1A3/EAAT1, SLC29A1/ENT1, and SLC38A3/SNAT3 (Figure S2). Notably, immunoblotting also detected transporters undetectable or below quantitation limits in proteomics, such as ABCC4, OATP1A2, OATP2B1, OAT3, SLC1A5, SLC6A14, SLC7A1, SLC7A3, and SLC7A11. These discrepancies likely reflect methodological differences. Proteomics depends on tryptic peptide detection and can be limited by digestion efficiency, peptide ionization, or post-translational modifications,[16,17] whereas immunoblotting relies on antibody recognition, benefiting from signal amplification but susceptible to cross-reactivity or non-specific binding.[18–20] Detection by immunoblotting but not proteomics may indicate low abundance or poor peptide detectability, underscoring the value of using complementary approaches to accurately profile transporter expression in the NVU.

NVU Structure in the Human Normal Brain Cortex and Glioblastoma

Immunofluorescence confocal microscopy enabled high-resolution visualization of the spatial organization of endothelial cells, pericytes, astrocytes, and neurons, revealing a tightly structured NVU in the human brain cortex (Figure 3A). Microvessels of the human normal brain cortex

exhibited a continuous and well-defined endothelial cell layer, identified by CD31 immunolabeling, which clearly delineated the vascular lumen. Pericytes, labeled with NG2, were closely associated with the abluminal surface of the endothelium, consistent with their role in maintaining BBB integrity and regulating capillary function.[21,22] Astrocytic end-feet, visualized by GFAP immunostaining, almost completely enveloped the microvessels, forming the perivascular glial limitans, while neurons, identified by SYP labeling, were positioned in close proximity to the vascular structure, reflecting the neurovascular coupling.[23]

In contrast, GBM microvessels displayed a markedly disorganized NVU architecture (Figure 3B). The CD31-positive endothelial layer appeared discontinuous and irregular, reflecting aberrant angiogenesis characteristic of tumor vasculature.[24] NG2-staining pericyte coverage was substantially reduced and uneven, consistent with impaired pericyte recruitment in GBM contributing to BBB leakiness.[21] GFAP-positive astrocytic end-feet were disorganized and frequently detached from the vascular wall, further compromising BBB integrity.[25] Interestingly, SYP staining associated with microvessels appeared enhanced, potentially reflecting aberrant synaptic remodeling or tumor-associated neuronal hyperactivity within the perivascular niche.[26]

Transporter Localization in the NVU

Immunofluorescence confocal microscopy enabled high-resolution visualization and quantitative assessment

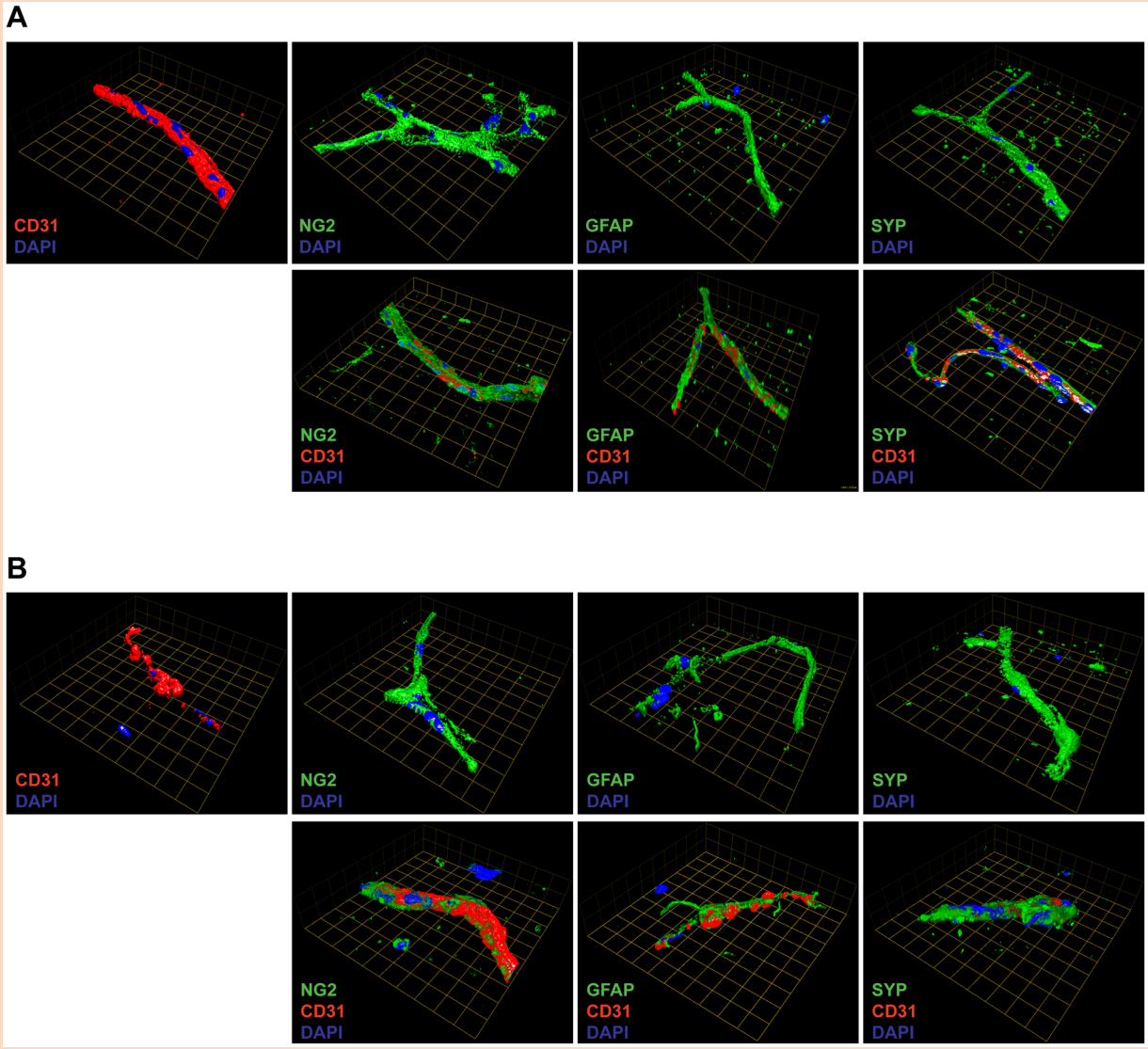

Figure 3 Immunofluorescence confocal microscopy visualization of the spatial organization of endothelial cells, pericytes, astrocytes, and neurons, revealing (A) a tightly structured neurovascular unit (NVU) in the human normal brain cortex and (B) a markedly disorganized NVU architecture in contrast-enhancing regions of GBM. Specific cell types were labeled with established cellular markers: platelet endothelial cell adhesion molecule-1 (PECAM-1 or CD31) for endothelial cells, glial fibrillary acidic protein (GFAP) for astrocytes, neural/glial antigen 2 (NG2) for pericytes, and synaptophysin (SYP) for neurons.

of transporter localization within distinct NVU cell types. Key transporters identified by targeted proteomics and immunoblotting, including ABCB1, ABCG2, Na^+/K^+-ATPase, GLUT1, GLUT3, LAT1, SLC1A2/EAAT2, SLC1A3/EAAT1, SLC29A1/ENT1, and SLC38A3/SNAT3, were evaluated. Two-dimensional images of single- and dual-immunofluorescent staining of individual transporters alongside individual cell-specific markers (CD31 for endothelial cells, NG2 for pericytes, GFAP for astrocytes, and SYP for neurons) confirmed antibody specificity and absence of cross-reactivity (Figure S3). Three-dimensional reconstructions of confocal z-stacks delineated the spatial distribution of individual transporters within the NVU of the human normal brain cortex (Figure 4). Semi-quantitative co-localization analysis using Manders' overlap coefficients (M1 and M2) and Pearson's correlation coefficients (Table 2) revealed distinct transporter localization patterns within the NVU of the human normal brain cortex.

ABCB1 was enriched in endothelial cells and astrocytes, whereas ABCG2 was broadly expressed across all NVU cell types. GLUT1 and GLUT3 were primarily localized to endothelial cells and astrocytes, with lower levels in pericytes and neurons. LAT1 strongly co-localized with endothelial cells and astrocytes. EAAT1 was enriched in pericytes and astrocytes, whereas EAAT2 primarily localized in endothelial cells. ENT1 was broadly distributed with enrichment in pericytes and astrocytics, while SNAT3 and Na^+/K^+-ATPase showed widespread distribution across all NVU cell types.

GBM microvessels exhibited a markedly disorganized NVU architecture (Figure S4). The cell-specific localization of individual transporters within distinct NVU components was substantially disrupted, displaying diffuse distribution patterns and reduced co-localization with endothelial cells, pericytes, and astrocytic end-feet (Figure S4). Such alterations are consistent with impaired barrier integrity, attenuated drug efflux capacity, and dysregulated nutrient and metabolite transport within tumor vasculature.[27,28] Collectively, these analyses emphasize the cell-type–specific expression of transporters in the NVU of the normal brain cortex and reveal tumor-associated alterations of transporter expression and localization within the GBM NVU.

Discussion

This study provides a comprehensive quantitative analysis of transporter protein expressions and cell-specific localization within the NVU of the normal human brain cortex, the non-cancerous cortex of GBM patients, and GBM tissue. By integrating targeted proteomics with high-resolution confocal immunofluorescence microscopy, we demonstrate marked disorganization of NVU architecture and aberrant transporter expression in GBM-associated microvessels. These findings provide mechanistic insights into NVU remodeling at both structural and molecular levels and underscore the contribution of altered transporter expression and localization to pharmacokinetic heterogeneity and metabolic reprogramming in GBM.

The barrier integrity of the NVU in GBM is known to be variably disrupted, ranging from completely compromised in bulk tumor regions, to moderately "leaky" in invasive margins, and fully intact in infiltrative areas.[28,29] This heterogeneity leads to large inter- and intra-individual pharmacokinetics variability in GBM. While drug penetration into bulk tumor regions is often enhanced, insufficient penetration of therapeutic agents into infiltrating regions behind an intact BBB remains a major obstacle to long-term, efficacious treatment of GBM.[28,29] Our targeted proteomics and confocal immunofluorescence analyses revealed that ABCB1 and ABCG2 are the predominant efflux transporters in the NVU of the human normal brain cortex. ABCB1 was primarily localized to endothelial cells and perivascular astrocytic endfeet, whereas ABCG2 was broadly distributed across multiple NVU cell types (Figure 4 and Table 2). These findings support the cooperative roles of ABCB1 and ABCG2 in maintaining NVU barrier integrity and restricting drug entry across the intact BBB.[30,31] Notably, despite extensive efforts, clinical trials using ABCB1 inhibitors to enhance drug brain delivery have largely failed, yielding limited improvements in brain penetration or efficacy, while causing intolerable toxicities and systemic pharmacokinetic interactions.[32] This limited success is largely attributable to the inability to achieve unbound plasma inhibitor concentrations sufficient for effective transporter inhibition in humans.[32] Furthermore, because ABCB1 and ABCG2 act synergistically to restrict drug brain delivery, inhibition of ABCB1 alone is unlikely to be an effective strategy for enhancing brain delivery of therapeutic drugs, many of which are dual substrates of ABCB1 and ABCG2.

Quantitative targeted proteomics showed that the protein abundance of ABCB1 and ABCG2 was largely preserved in microvessels isolated from both contrast-enhancing and non-enhancing regions of human GBM compared with those from normal brain cortex (Figure 2). On the other hand, confocal immunofluorescence microscopy revealed marked disruption of NVU architecture and mislocalized expression of ABCB1 and ABCG2 in microvessels isolated from contrast-enhancing regions (Figure 3 and Figure S4). Collectively, the disorganized NVU structural and mislocalized efflux transporters likely leads to diminished or absent active efflux function of ABCB1 and ABCG2 in these regions, providing mechanistic insight into the clinically observed enhanced penetration of ABCB1/ABCG2 substrate drugs into contrast-enhancing GBM lesions.[33–35] Conversely, ABCB1 and ABCG2 efflux function is likely retained, for a large part, in the NVU of non-enhancing tumor regions as the NVU structure and efflux transporter expression and localization appeared largely preserved in these regions. This is consistent with clinical evidence showing significantly lower penetration of ABCB1/ABCG2 substrate drugs into non-enhancing, infiltrative tumor areas compared with contrast-enhancing regions in GBM patients.[33–35] Effective long-term treatment of GBM relies on achieving sufficient drug exposure within infiltrative tumor regions, which are often unresectable and responsible for recurrence. However, many preclinical and clinical studies only measure drug concentrations in contrast-enhancing regions, overlooking the non-enhancing areas. Assessment of drug penetration and exposure in non-enhancing regions is essential, as such quantitative data can provide critical insights to guide the selection of effective therapeutic agents and optimization of dosing regimens for improved treatment outcomes.

Targeted proteomics revealed marked alterations in transporter protein abundance in microvessels isolated from both

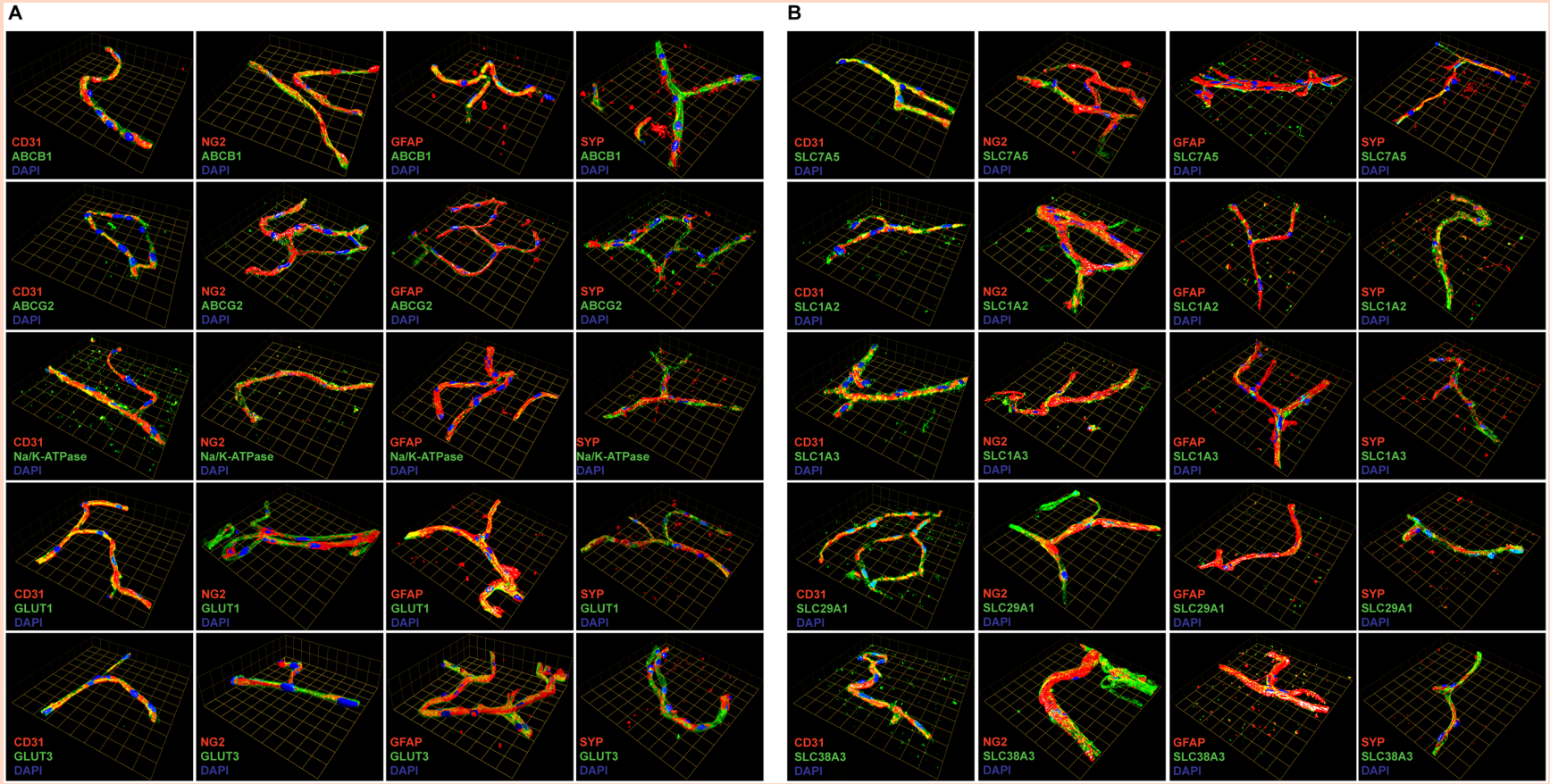

Figure 4 Immunofluorescence confocal microscopy visualization of the localization of individual transporters (including ABCB1, ABCG2, Na^+/K^+-ATPase, GLUT1, GLUT3, LAT1, EAAT2, EAAT1, ENT1, and SNAT3) within distinct cell compartments of the neurovascular unit in the human normal brain cortex. Specific cell types were labeled with established cellular markers: platelet endothelial cell adhesion molecule-1 (PECAM-1 or CD31) for endothelial cells, glial fibrillary acidic protein (GFAP) for astrocytes, neural/glial antigen 2 (NG2) for pericytes, and synaptophysin (SYP) for neurons.

Table 2. Quantitative data summarizing the extent of transporter co-localization across different cell types in the neurovascular unit of the human normal brain cortex[a]

	Endothelial cells (CD31)			Pericytes (NG2)			Astrocytes (GFAP)			Neurons (SYP)		
	M1[b]	M2[c]	PCC[d]	M1[b]	M2[c]	PCC[d]	M1[b]	M2[c]	PCC[d]	M1[b]	M2[c]	PCC[d]
ABCB1	0.90 (1.8%)	0.43 (4.3%)	0.35 (3.1%)	0.41 (32.2%)	0.39 (19.9%)	0.06 (11.6%)	0.94 (3.9%)	0.24 (5.9%)	0.34 (6.7%)	0.43 (10.9%)	0.25 (11.1%)	0.09 (37.5%)
ABCG2	0.71 (10.5%)	0.27 (22.5%)	0.11 (17.8%)	0.42 (22.9%)	0.42 (6.8%)	0.10 (44.5%)	0.76 (11.2%)	0.30 (16.4%)	0.15 (34.7%)	0.33 (9.5%)	0.41 (13.3%)	0.25 (21.8%)
Na/K ATPase	0.54 (11.7%)	0.68 (5.8%)	0.06 (52.8%)	0.35 (11.3%)	0.60 (22.4%)	0.14 (26.8%)	0.82 (3.4%)	0.66 (16.3%)	0.29 (18.9%)	0.35 (12.1%)	0.60 (8.9%)	0.27 (22.2%)
SLC2A1 (GLUT1)	0.88 (6.1%)	0.40 (26.0%)	0.40 (36.3%)	0.47 (48.8%)	0.41 (24.6%)	0.15 (28.3%)	0.88 (5.4%)	0.46 (23.9%)	0.30 (23.3%)	0.52 (19.3%)	0.54 (19.5%)	0.09 (12.4%)
SLC2A3 (GLUT3)	0.82 (5.1%)	0.43 (20.2%)	0.33 (10.9%)	0.40 (19.0%)	0.41 (9.8%)	0.10 (37.9%)	0.91 (1.0%)	0.46 (22.8%)	0.32 (25.0%)	0.41 (3.3%)	0.38 (12.1%)	0.11 (45.7%)
SLC7A5 (LAT1)	0.76 (8.5%)	0.42 (14.7%)	0.20 (34.4%)	0.35 (11.9%)	0.34 (12.3%)	0.02 (48.5%)	0.85 (4.0%)	0.58 (5.2%)	0.32 (8.1%)	0.43 (15.9%)	0.52 (12.3%)	0.08 (3.4%)
SLC1A2 (EAAT2)	0.72 (2.2%)	0.30 (15.4%)	0.28 (17.4%)	0.64 (10.3%)	0.28 (15.6%)	0.17 (19.4%)	0.79 (3.3%)	0.49 (13.8%)	0.19 (25.9%)	0.41 (24.1%)	0.35 (17.0%)	0.13 (18.5%)
SLC1A3 (EAAT1)	0.37 (5.6%)	0.19 (0.8%)	0.002 (0%)	0.58 (5.4%)	0.47 (17.9%)	0.28 (8.1%)	0.77 (9.8%)	0.29 (24.3%)	0.25 (57.7%)	0.33 (12.8%)	0.20 (46.4%)	0.07 (10.3%)
SLC29A1 (ENT1)	0.67 (6.5%)	0.38 (11.9%)	0.07 (18.7%)	0.60 (4.4%)	0.56 (19.2%)	0.21 (14.8%)	0.90 (3.4%)	0.50 (13.5%)	0.23 (32.2%)	0.44 (10.3%)	0.42 (15.8%)	0.12 (32.5%)
SLC38A3 (SNAT3)	0.75 (5.5%)	0.58 (15.7%)	0.20 (0.8%)	0.44 (15.2%)	0.65 (5.2%)	0.15 (12.9%)	0.84 (5.5%)	0.73 (9.1%)	0.36 (19.0%)	0.46 (6.9%)	0.65 (8.7%)	0.26 (33.2%)

[a]Data are shown as the mean (with coefficient variation%) from 4 or 5 regions of interest.
[b]M1, Mander's overlap coefficient representing the percentage of pixels in Channel 1 (transporter) that overlap with Channel 2 (cell marker).
[c]M2, Mander's overlap coefficient representing the percentage of pixels in Channel 2 (cell marker) that overlap with Channel 1 (transporter).
[d]PCC, Pearson's correlation coefficient assessing the degree of signal correlation between the transporter and cell marker channels.

non-enhancing and enhancing regions of GBM, compared with normal brain cortex (Figure 2 and Table 1). While ABC efflux transporters (ABCB1, ABCG2) were largely preserved, ion and nutrient transporters (Na^+/K^+-ATPase, GLUT3, EAAT1, EAAT2, SNAT2) were significantly reduced (ANOVA, $P<.05$). GLUT1 appeared downregulated while not reaching statistical significance. LAT1 and SNAT3 protein abundance was significantly increased (ANOVA, $P<.05$). Notably, despite substantial inter-individual variability (Figure S1), the overall mean or median abundances of all detectable transporters did not differ significantly between the paired non-enhancing and contrast-enhancing regions of GBM (ANOVA, $P>.05$) (Figure 2 and Table 1). Given that the NVU structure and physical barrier are largely preserved in non-enhancing regions, as evidenced by the limited penetration of MRI contrast agents,[29,36] the observed transporter dysregulation in these regions suggests that biochemical barrier alterations may precede overt structural disruption of the NVU. Such early molecular changes may reflect and facilitate the metabolic reprogramming and adaptability of infiltrative tumor cells through selective regulation of nutrient and ion transporters.

It should be emphasized that non-enhancing tumor regions are clinically significant, as they are often surgically unresectable or represent post-surgical residual disease and are routinely exposed to radiotherapy and/or chemotherapy. An increasing body of evidence indicates that radiotherapy and chemotherapy can induce inflammatory signaling, endothelial injury, and NVU remodeling, leading to dysregulation of transporter expression and subcellular localization within the NVU of non-enhancing tumor regions.[37–40] Such alterations may have important clinical implications for drug delivery, therapeutic resistance, tumor recurrence, and imaging phenomena such as pseudoprogression. Although this study did not directly investigate treatment-induced effects on transporter protein expression and localization in the NVU, due to the small sample size and pooled samples from both untreated and treated GBM patients, this represents an important direction for future studies.

Brain function critically depends on glucose as its primary energy substrate, requiring transport across the BBB and subsequently into glial cells and neurons. More than 10 members of the GLUT gene family contribute to glucose transport within the NVU and brain parenchyma.[41] Among them, GLUT1 is the predominant transporter in brain microvessels, whereas GLUT3 is mainly localized to non-vascular cells and, to a lesser extent, isolated microvessels.[41,42] Consistent with this, our targeted proteomics showed that GLUT1 abundance in human normal cortex microvessels was approximately twice that of GLUT3 (median, 28.4 vs. 14.9 fmol/μg protein; Table 1). Confocal imaging further confirmed their localization to endothelial cells and astrocytic endfeet of the NVU (Figure 4), in agreement with prior observations.[41]

Compared with that in normal brain cortex microvessels, median GLUT1 abundance decreased by 25% and 42% (not statistically significant, ANOVA, $P>.05$) in non-enhancing and contrast-enhancing GBM regions, respectively, whereas GLUT3 abundance declined significantly by 87% and 78% (ANOVA, $P<.0001$) in these regions, respectively (Figure 2 and Table 1). These findings corroborate earlier immunocytochemical and proteomic studies reporting diminished

GLUT1 and GLUT3 expression in microvessels of human brain tumors.[8,15,43,44] The observed reductions in GLUT1 and GLUT3 protein expressions in both non-enhancing and enhancing GBM regions are unexpected, given the elevated glycolytic demand of malignant tumors.[45,46] One possible explanation is that glucose, being water-soluble, may partially diffuse through the leaky tight junctions of the blood-brain tumor barrier via passive paracellular transport, thereby reducing the dependence on facilitated transporter-mediated uptake.[43,44] Further studies are needed to clarify the mechanisms governing GLUT1 and GLUT3 regulation within the GBM NVU.

LAT1 is the most abundant amino acid carrier localized on both the luminal and abluminal membranes of brain capillary endothelial cells.[47,48] It mediates the sodium-independent transport of large neutral amino acids (including leucine, isoleucine, valine, tryptophan, tyrosine, and phenylalanine) as well as several pharmacologically relevant substrates (e.g., L-dopa, melphalan, gabapentin, and baclofen) across the BBB.[49,50] Confocal immunofluorescence microscopy revealed that LAT1 was predominantly localized in endothelial cells and astrocyte endfeet within the NVU of normal brain cortex (Figure 4 and Table 2), highlighting its critical role in facilitating amino acid exchange across the BBB and supporting amino acid metabolism within the NVU. Targeted proteomics determined that median LAT1 protein abundance was approximately 2-fold higher in microvessels isolated from both non-enhancing and enhancing regions of GBM (3.68 and 3.24 fmol/μg protein, respectively) compared with that in normal cortex microvessels (1.68 fmol/μg protein; ANOVA, $P < .01$; Figure 2 and Table 1). This upregulation agrees with previous reports of elevated LAT1 expression in brain tumor microvessels and aligns with the increased amino acid demand of rapidly proliferating glioma cells.[51,52]

Excitatory amino acid transporters (EAAT1 and EAAT2), the most abundant subtypes of glutamate transporters in the CNS, play a pivotal role in regulation of neurotransmission by clearing the excitatory neurotransmitter glutamate from the extracellular space at synapses.[53,54] Confocal immunofluorescence microscopy demonstrated that within the NVU of normal brain cortex, EAAT1 was predominantly localized in pericytes and astrocytes, whereas EAAT2 showed broader expression across all NVU cell types with a primary enrichment in endothelial cells (Figure 4 and Table 2). These findings suggest that EAAT1 and EAAT2 may have complementary and coordinated functions in maintaining neurovascular metabolic coupling within the NVU. Targeted proteomics revealed that the median protein abundances of EAAT1 and EAAT2 in microvessels isolated from both non-enhancing and enhancing regions of GBM were reduced to less than 15% of their levels in normal brain cortex microvessels (ANOVA, $P < .05$; Figure 2 and Table 1). Dysfunction of EAAT1 and EAAT2 has been implicated in several neuropathological conditions such as traumatic brain injury, stroke, Amyotrophic lateral sclerosis, and Alzheimer's disease.[53,54] The pronounced downregulation of EAAT1 and EAAT2 observed in GBM-associated NVU may therefore contribute to impaired neurovascular metabolic coupling, potentially facilitating tumor cell invasion and progression.

SNAT2 and SNAT3 are sodium-coupled neutral amino acid transporters belonging to distinct functional subfamilies. SNAT2 acts as a System A transporter preferring small neutral amino acids such as alanine, whereas SNAT3 functions as a System N transporter selective for glutamine, asparagine, and histidine.[55] In the brain, SNAT2 is primarily neuronal and supports the glutamate-GABA-glutamine cycle by mediating glutamine uptake into glutamatergic and GABAergic neurons.[56] SNAT3, in contrast, is mainly localized in astrocytes and endothelial cells of the BBB. Consistent with this distribution, our confocal immunofluorescence microscopy revealed enrichment of SNAT3 in endothelial cells and astrocyte endfeet within the NVU of the normal brain cortex (Figure 4 and Table 2). SNAT3 likely serves as the principal System N transporter regulating glutamine flux across the BBB, with directionality determined by brain interstitial glutamine levels.[57–59] In addition to its BBB role, SNAT3 contributes to neurotransmission by involving in the astrocyte-neuron glutamate-glutamine cycle, where astrocytes clear synaptic glutamate via EAAT1/2, convert it to glutamine, and release it through SNAT3, and subsequently neurons take up glutamine primarily via SNAT1/2 and convert it back to glutamate to replenish neurotransmitter pools.[55] Targeted proteomics revealed pronounced alterations in SNAT expression in GBM microvessels. SNAT2 protein levels were markedly reduced or undetectable, whereas SNAT3 expression was significantly upregulated in both non-enhancing and enhancing tumor regions (ANOVA, $P < .05$; Figure 2 and Table 1). The loss or reduction of SNAT2 in GBM NVU may reflect disrupted neurovascular coupling, while upregulated SNAT3 likely represents an adaptive response to the heightened glutamine requirement of proliferating GBM cells.

Equilibrative nucleoside transporter 1 (ENT1) is a bidirectional, sodium-independent transporter that mediates cellular uptake and release of nucleosides such as adenosine. In the brain, ENT1 is primarily neuronal and is also present in human brain capillary.[17,60,61] Consistent with this, our confocal immunofluorescence microscopy showed ENT1 broad distribution across NVU cell types in normal brain cortex, with notable enrichment in pericytes and astrocyte endfeet (Figure 4 and Table 2), supporting its role in maintaining adenosine hemostasis of the NVU and potentially mediating purine/pyrimidine transport across the BBB. Targeted proteomics revealed that ENT1 median abundance in microvessels from both non-enhancing and enhancing GBM regions was reduced to <25% of its level in normal brain cortex microvessels (ANOVA, $P < .001$; Figure 2 and Table 1). Reduced ENT1 expression has been linked to elevated extracellular adenosine in GBM, promoting immunosuppression, angiogenesis, and tumor progression.[62,63] Altered ENT1 expression in GBM NVU may also impair BBB transport, contribute to vascular dysfunction, and influence responsiveness to nucleoside analog chemotherapies. Given its essential role in nucleoside balance and neuromodulatory signaling, ENT1 dysregulation likely supports a tumor-favorable microenvironment and therapeutic resistance.

Na^+/K^+-ATPase, a membrane-bound enzyme complex comprising catalytic α- and regulatory β-subunits, maintains ionic gradients essential for neuronal excitability and cerebrovascular homeostasis. Consistent with earlier studies,[64,65]

our confocal immunofluorescence microscopy showed broad Na^+/K^+-ATPase expression across all NVU cell types in the normal brain cortex, including neurons, astrocytes, endothelial cells, and pericytes (Figure 4 and Table 2). Within the NVU, α1 and β1/β3 isoforms predominate in endothelial cells, supporting trans-BBB ion transport and osmotic regulation,[66] whereas astrocytic α2 and β2 isoforms are enriched at perivascular end-feet, contributing to K^+ buffering, neurovascular coupling, and BBB stability.[67] Neurons predominantly express the α3 isoform to meet rapid ionic demands during action potentials and synaptic transmission.[68] In GBM, Na^+/K^+-ATPase expression and subunit localization are frequently disrupted. Several studies have reported downregulation of α2 and β2 subunits in tumor and peritumoral astrocytes, resulting in compromised ionic balance, peritumoral edema, and increased excitotoxic stress.[67,69] Consistent with this, our targeted proteomics showed that Na^+/K^+-ATPase abundance in microvessels from both non-enhancing and contrast-enhancing tumor regions was reduced to ~20% of the level in normal cortex microvessels (ANOVA, $P<.0001$; Figure 2 and Table 1). The marked downregulation of Na^+/K^+-ATPase in GBM microvessels likely contributes to disrupted ion homeostasis, impaired BBB function, and the invasive phenotype of GBM.

In summary, our integrative analysis demonstrates that GBM profoundly remodels the human NVU at both structural and molecular levels. The disruption of transporter protein expression and cell-specific localization reflects a breakdown of the coordinated neurovascular and metabolic coupling that are essential to NVU function. These alterations likely contribute to the pharmacokinetic heterogeneity, metabolic reprogramming, and invasive characteristics of GBM. Therapeutic strategies that address both NVU dysfunction and transporter dysregulation may improve drug delivery and harness metabolic vulnerability in GBM.

Supplementary Material

Supplementary material is available online at *Neuro-Oncology Advances* (https://academic.oup.com/noa).

Keywords

confocal immunofluorescence microscopy | glioblastoma | neurovascular unit (NVU) | quantitative targeted proteomics | transporters

Author Contributions

Study concept and design: J.L. Implementation, data analysis and interpretation: J.L., X.B., Y.J., N.S., B.H. All authors have been involved in the writing of the manuscript and have read and approved of the final version.

Conflict of Interest

All authors declared no competing interests for this work.

Funding

The National Cancer Institute of the National Institute of Health (NIH) R01CA255124 to J.L. and NIH Cancer Center Support Grant P30CA022453 (Karmanos Cancer Institute Pharmacology and Metabolomics Core).

Acknowledgments

We would like to thank Kamiar Moin, PhD, and Linda Mayernik in the Wayne State University Imaging Core for their technical support for confocal immunofluorescence microscopy.

Data Availability

Data presented in the manuscript and supplementary file are available to readers.

Affiliations

Karmanos Cancer Institute, Wayne State University School of Medicine, Detroit, Michigan, USA (X.B., Y.J., J.L.); Barrow Neurological Institute, St. Joseph's Hospital & Medical Center, Phoenix, Arizona, USA (B.H., N.S.)

References

1. McConnell HL, Kersch CN, Woltjer RL, Neuwelt EA. The translational significance of the neurovascular unit. *J Biol Chem*. 2017;292:762-770. https://doi.org/10.1074/jbc.R116.760215
2. McConnell HL, Mishra A. Cells of the blood–brain barrier: an overview of the neurovascular unit in health and disease. *Methods Mol Biol*. 2022;2492:3-24. https://doi.org/10.1007/978-1-0716-2289-6_1
3. Lee J, Lund-Smith C, Borboa A, Gonzalez AM, Baird A, Eliceiri BP. Glioma-induced remodeling of the neurovascular unit. *Brain Res*. 2009;1288:125-134. https://doi.org/10.1016/j.brainres.2009.06.095
4. Pombero A, Garcia-Lopez R, Martinez S. Pericyte-Glioblastoma cell interaction: a key target to prevent glioblastoma progression. *Cells*. 2023;12:1324. https://doi.org/10.3390/cells12091324
5. Ohtsuki S, Schaefer O, Kawakami H, et al. Simultaneous absolute protein quantification of transporters, cytochromes P450, and UDP-glucuronosyltransferases as a novel approach for the characterization of individual human liver: comparison with mRNA levels and activities.

Drug Metab Dispos. 2012;40:83-92. https://doi.org/10.1124/dmd.111.042259
6. Wang D, Eraslan B, Wieland T, et al. A deep proteome and transcriptome abundance atlas of 29 healthy human tissues. *Mol Syst Biol*. 2019;15:e8503. https://doi.org/10.15252/msb.20188503
7. Beck WT, Grogan TM, Willman CL, et al. Methods to detect P-glycoprotein-associated multidrug resistance in patients' tumors: consensus recommendations. *Cancer Res*. 1996;56:3010-3020.
8. Bao X, Wu J, Jiang J, Tien AC, Sanai N, Li J. Quantitative protein expression of blood–brain barrier transporters in the vasculature of brain metastases of patients with lung and breast cancer. *Clin Transl Sci*. 2021;14:1265-1271. https://doi.org/10.1111/cts.12978
9. Bernard-Patrzynski F, Lecuyer MA, Puscas I, et al. Isolation of endothelial cells, pericytes and astrocytes from mouse brain. *PLoS One*. 2019;14:e0226302. https://doi.org/10.1371/journal.pone.0226302
10. Birbrair A, Zhang T, Files DC, et al. Type-1 pericytes accumulate after tissue injury and produce collagen in an organ-dependent manner. *Stem Cell Res Ther*. 2014;5:122. https://doi.org/10.1186/scrt512
11. Huang H, He W, Tang T, Qiu M. Immunological markers for central nervous system glia. *Neurosci Bull*. 2023;39:379-392. https://doi.org/10.1007/s12264-022-00938-2
12. Wiedenmann B, Franke WW. Identification and localization of synaptophysin, an integral membrane glycoprotein of Mr 38,000 characteristic of presynaptic vesicles. *Cell*. 1985;41:1017-1028. https://doi.org/10.1016/s0092-8674(85)80082-9
13. Dunn KW, Kamocka MM, McDonald JH. A practical guide to evaluating colocalization in biological microscopy. *Am J Physiol Cell Physiol*. 2011;300:C723-C742. https://doi.org/10.1152/ajpcell.00462.2010
14. Zinchuk V, Zinchuk O, Okada T. Quantitative colocalization analysis of multicolor confocal immunofluorescence microscopy images: pushing pixels to explore biological phenomena. *Acta Histochem Cytochem*. 2007;40:101-111. https://doi.org/10.1267/ahc.07002
15. Bao X, Wu J, Xie Y, et al. Protein expression and functional relevance of efflux and uptake drug transporters at the blood–brain barrier of human brain and glioblastoma. *Clin Pharmacol Ther*. 2020;107:1116-1127. https://doi.org/10.1002/cpt.1710
16. Gallien S, Duriez E, Domon B. Selected reaction monitoring applied to proteomics. *J Mass Spectrom*. 2011;46:298-312. https://doi.org/10.1002/jms.1895
17. Uchida Y, Ohtsuki S, Katsukura Y, et al. Quantitative targeted absolute proteomics of human blood–brain barrier transporters and receptors. *J Neurochem*. 2011;117:333-345. https://doi.org/10.1111/j.1471-4159.2011.07208.x
18. Mahmood T, Yang PC. Western blot: technique, theory, and trouble shooting. *N Am J Med Sci*. 2012;4:429-434. https://doi.org/10.4103/1947-2714.100998
19. Baker M. Reproducibility crisis: blame it on the antibodies. *Nature*. 2015;521:274-276. https://doi.org/10.1038/521274a
20. Bordeaux J, Welsh A, Agarwal S, et al. Antibody validation. *Biotechniques*. 2010;48:197-209. https://doi.org/10.2144/000113382
21. Armulik A, Genove G, Mae M, et al. Pericytes regulate the blood–brain barrier. *Nature*. 2010;468:557-561. https://doi.org/10.1038/nature09522
22. Daneman R, Prat A. The blood–brain barrier. *Cold Spring Harb Perspect Biol*. 2015;7:a020412. https://doi.org/10.1101/cshperspect.a020412
23. Iadecola C. The neurovascular unit coming of age: a journey through neurovascular coupling in health and disease. *Neuron*. 2017;96:17-42. https://doi.org/10.1016/j.neuron.2017.07.030
24. Hardee ME, Zagzag D. Mechanisms of glioma-associated neovascularization. *Am J Pathol*. 2012;181:1126-1141. https://doi.org/10.1016/j.ajpath.2012.06.030
25. Quail DF, Joyce JA. The microenvironmental landscape of brain tumors. *Cancer Cell*. 2017;31:326-341. https://doi.org/10.1016/j.ccell.2017.02.009
26. Venkatesh HS, Johung TB, Caretti V, et al. Neuronal activity promotes glioma growth through neuroligin-3 secretion. *Cell*. 2015;161:803-816. https://doi.org/10.1016/j.cell.2015.04.012
27. Watkins S, Robel S, Kimbrough IF, Robert SM, Ellis-Davies G, Sontheimer H. Disruption of astrocyte-vascular coupling and the blood–brain barrier by invading glioma cells. *Nat Commun*. 2014;5:4196. https://doi.org/10.1038/ncomms5196
28. Arvanitis CD, Ferraro GB, Jain RK. The blood–brain barrier and blood–tumour barrier in brain tumours and metastases. *Nat Rev Cancer*. 2020;20:26-41. https://doi.org/10.1038/s41568-019-0205-x
29. Sarkaria JN, Hu LS, Parney IF, et al. Is the blood–brain barrier really disrupted in all glioblastomas? A critical assessment of existing clinical data. *Neuro Oncol*. 2018;20:184-191. https://doi.org/10.1093/neuonc/nox175
30. Agarwal S, Hartz AM, Elmquist WF, Bauer B. Breast cancer resistance protein and P-glycoprotein in brain cancer: two gatekeepers team up. *Curr Pharm Des*. 2011;17:2793-2802. https://doi.org/10.2174/138161211797440186
31. Loscher W, Potschka H. Role of drug efflux transporters in the brain for drug disposition and treatment of brain diseases. *Prog Neurobiol*. 2005;76:22-76. https://doi.org/10.1016/j.pneurobio.2005.04.006
32. Kalvass JC, Polli JW, Bourdet DL, et al.; International Transporter Consortium. Why clinical modulation of efflux transport at the human blood–brain barrier is unlikely: the ITC evidence-based position. *Clin Pharmacol Ther*. 2013;94:80-94. https://doi.org/10.1038/clpt.2013.34
33. Li J, Wickramasinghe C, Jiang J, et al. Mechanistic modeling of spatial heterogeneity of drug penetration and exposure in the human central nervous system and brain tumors. *Clin Pharmacol Ther*. 2025;117:690-703. https://doi.org/10.1002/cpt.3505
34. Sanai N, Li J, Boerner J, et al. Phase 0 trial of AZD1775 in first-recurrence glioblastoma patients. *Clin Cancer Res*. 2018;24:3820-3828. https://doi.org/10.1158/1078-0432.CCR-17-3348
35. Tien AC, Li J, Bao X, et al. A phase 0 trial of ribociclib in recurrent glioblastoma patients incorporating a tumor pharmacodynamic- and pharmacokinetic-guided expansion cohort. *Clin Cancer Res*. 2019;25:5777-5786. https://doi.org/10.1158/1078-0432.CCR-19-0133
36. John F, Robinette NL, Amit-Yousif AJ, et al. Multimodal imaging of non-enhancing glioblastoma regions. *Mol Imaging*. 2019;18:1536012119885222. https://doi.org/10.1177/1536012119885222
37. Allen BD, Limoli CL. Breaking barriers: neurodegenerative repercussions of radiotherapy induced damage on the blood–brain and blood–tumor barrier. *Free Radic Biol Med*. 2022;178:189-201. https://doi.org/10.1016/j.freeradbiomed.2021.12.002
38. Blethen KE, Sprowls SA, Arsiwala TA, et al. Effects of whole-brain radiation therapy on the blood–brain barrier in immunocompetent and immunocompromised mouse models. *Radiat Oncol*. 2023;18:22. https://doi.org/10.1186/s13014-023-02215-6
39. Ren X, Boriero D, Chaiswing L, Bondada S, St Clair DK, Butterfield DA. Plausible biochemical mechanisms of chemotherapy-induced cognitive impairment ("chemobrain"), a condition that significantly impairs the quality of life of many cancer survivors. *Biochim Biophys Acta Mol Basis Dis*. 2019;1865:1088-1097. https://doi.org/10.1016/j.bbadis.2019.02.007
40. Zhang W, Grams MP, Oberoi RK, et al. The impact of therapeutic radiation on drug distribution across the blood–brain barrier in normal mouse brain and orthotopic glioblastoma tumors. *Neuro Oncol*. 2025;27:2250-2261. https://doi.org/10.1093/neuonc/noaf093
41. Patching SG. Glucose transporters at the blood–brain barrier: function, regulation and gateways for drug delivery. *Mol Neurobiol*. 2017;54:1046-1077. https://doi.org/10.1007/s12035-015-9672-6
42. Gerhart DZ, Broderius MA, Borson ND, Drewes LR. Neurons and microvessels express the brain glucose transporter protein GLUT3. *Proc*

Natl Acad Sci U S A. 1992;89:733-737. https://doi.org/10.1073/pnas.89.2.733

43. Guerin C, Laterra J, Hruban RH, Brem H, Drewes LR, Goldstein GW. The glucose transporter and blood–brain barrier of human brain tumors. *Ann Neurol*. 1990;28:758-765. https://doi.org/10.1002/ana.410280606
44. Harik SI, Roessmann U. The erythrocyte-type glucose transporter in blood vessels of primary and metastatic brain tumors. *Ann Neurol*. 1991;29:487-491. https://doi.org/10.1002/ana.410290507
45. Di Chiro G, DeLaPaz RL, Brooks RA, et al. Glucose utilization of cerebral gliomas measured by [^{18}F] fluorodeoxyglucose and positron emission tomography. *Neurology*. 1982;32:1323-1329. https://doi.org/10.1212/wnl.32.12.1323
46. Mangiardi JR, Yodice P. Metabolism of the malignant astrocytoma. *Neurosurgery*. 1990;26:1-19. https://doi.org/10.1097/00006123-199001000-00001
47. Boado RJ, Li JY, Nagaya M, Zhang C, Pardridge WM. Selective expression of the large neutral amino acid transporter at the blood–brain barrier. *Proc Natl Acad Sci U S A*. 1999;96:12079-12084. https://doi.org/10.1073/pnas.96.21.12079
48. Duelli R, Enerson BE, Gerhart DZ, Drewes LR. Expression of large amino acid transporter LAT1 in rat brain endothelium. *J Cereb Blood Flow Metab*. 2000;20:1557-1562. https://doi.org/10.1097/00004647-200011000-00005
49. Kageyama T, Nakamura M, Matsuo A, et al. The 4F2hc/LAT1 complex transports L-DOPA across the blood–brain barrier. *Brain Res*. 2000;879:115-121. https://doi.org/10.1016/s0006-8993(00)02758-x
50. Gynther M, Laine K, Ropponen J, et al. Large neutral amino acid transporter enables brain drug delivery via prodrugs. *J Med Chem*. 2008;51:932-936. https://doi.org/10.1021/jm701175d
51. Kido Y, Tamai I, Uchino H, Suzuki F, Sai Y, Tsuji A. Molecular and functional identification of large neutral amino acid transporters LAT1 and LAT2 and their pharmacological relevance at the blood–brain barrier. *J Pharm Pharmacol*. 2001;53:497-503. https://doi.org/10.1211/0022357011775794
52. Ahmed HS. The multifaceted role of L-type amino acid transporter 1 at the blood–brain barrier: structural implications and therapeutic potential. *Mol Neurobiol*. 2025;62:3813-3832. https://doi.org/10.1007/s12035-024-04506-9
53. Jensen AA, Fahlke C, Bjorn-Yoshimoto WE, Bunch L. Excitatory amino acid transporters: recent insights into molecular mechanisms, novel modes of modulation and new therapeutic possibilities. *Curr Opin Pharmacol*. 2015;20:116-123. https://doi.org/10.1016/j.coph.2014.10.008
54. Magi S, Piccirillo S, Amoroso S, Lariccia V. Excitatory amino acid transporters (EAATs): glutamate transport and beyond. *Int J Mol Sci*. 2019;20:5674. https://doi.org/10.3390/ijms20225674
55. Rubio-Aliaga I, Wagner CA. Regulation and function of the SLC38A3/SNAT3 glutamine transporter. *Channels (Austin)*. 2016;10:440-452. https://doi.org/10.1080/19336950.2016.1207024
56. Bak LK, Schousboe A, Waagepetersen HS. The glutamate/GABA-glutamine cycle: aspects of transport, neurotransmitter homeostasis and ammonia transfer. *J Neurochem*. 2006;98:641-653. https://doi.org/10.1111/j.1471-4159.2006.03913.x
57. Chan K, Busque SM, Sailer M, et al. Loss of function mutation of the Slc38a3 glutamine transporter reveals its critical role for amino acid metabolism in the liver, brain, and kidney. *Pflugers Arch*. 2016;468:213-227. https://doi.org/10.1007/s00424-015-1742-0
58. Ennis SR, Kawai N, Ren XD, Abdelkarim GE, Keep RF. Glutamine uptake at the blood–brain barrier is mediated by N-system transport. *J Neurochem*. 1998;71:2565-2573. https://doi.org/10.1046/j.1471-4159.1998.71062565.x
59. Ruderisch N, Virgintino D, Makrides V, Verrey F. Differential axial localization along the mouse brain vascular tree of luminal sodium-dependent glutamine transporters Snat1 and Snat3. *J Cereb Blood Flow Metab*. 2011;31:1637-1647. https://doi.org/10.1038/jcbfm.2011.21
60. Redzic ZB, Biringer J, Barnes K, et al. Polarized distribution of nucleoside transporters in rat brain endothelial and choroid plexus epithelial cells. *J Neurochem*. 2005;94:1420-1426. https://doi.org/10.1111/j.1471-4159.2005.03312.x
61. Alanko L, Porkka-Heiskanen T, Soinila S. Localization of equilibrative nucleoside transporters in the rat brain. *J Chem Neuroanat*. 2006;31:162-168. https://doi.org/10.1016/j.jchemneu.2005.12.001
62. Alarcon S, Toro MLA, Villarreal C, et al. Decreased equilibrative nucleoside transporter 1 (ENT1) activity contributes to the high extracellular adenosine levels in mesenchymal glioblastoma stem-like cells. *Cells*. 2020;9:1914. https://doi.org/10.3390/cells9081914
63. Allard B, Allard D, Buisseret L, Stagg J. The adenosine pathway in immuno-oncology. *Nat Rev Clin Oncol*. 2020;17:611-629. https://doi.org/10.1038/s41571-020-0382-2
64. Clausen MV, Hilbers F, Poulsen H. The structure and function of the Na,K-ATPase isoforms in health and disease. *Front Physiol*. 2017;8:371. https://doi.org/10.3389/fphys.2017.00371
65. D'Ambrosio R, Gordon DS, Winn HR. Differential role of KIR channel and Na(+)/K(+)-pump in the regulation of extracellular K(+) in rat hippocampus. *J Neurophysiol*. 2002;87:87-102. https://doi.org/10.1152/jn.00240.2001
66. Lykke K, Assentoft M, Horlyck S, et al. Evaluating the involvement of cerebral microvascular endothelial Na(+)/K(+)-ATPase and Na(+)-K(+)-2Cl(–) co-transporter in electrolyte fluxes in an in vitro blood–brain barrier model of dehydration. *J Cereb Blood Flow Metab*. 2019;39:497-512. https://doi.org/10.1177/0271678X17736715
67. Rotoli D, Cejas MM, Maeso MD, et al. The Na, K-ATPase beta-Subunit isoforms expression in glioblastoma multiforme: moonlighting roles. *Int J Mol Sci*. 2017;18:2369. https://doi.org/10.3390/ijms18112369
68. Richards KS, Bommert K, Szabo G, Miles R. Differential expression of Na+/K+-ATPase alpha-subunits in mouse hippocampal interneurones and pyramidal cells. *J Physiol*. 2007;585:491-505. https://doi.org/10.1113/jphysiol.2007.144733
69. Sun MZ, Kim JM, Oh MC, et al. Na (+)/K(+)-ATPase beta2-subunit (AMOG) expression abrogates invasion of glioblastoma-derived brain tumor-initiating cells. *Neuro Oncol*. 2013;15:1518-1531. https://doi.org/10.1093/neuonc/not099